Results from the C^+ Square-Degree Survey: Expanding Bubbles in Orion A

Cornelia Pabst

Leiden Observatory

August 19, 2020

in collaboration with:

J.R. Goicoechea, D. Teyssier, O. Berné, R.D. Higgins, E.T. Chambers, A. Hacar, M.G. Wolfire, S. Kabanovic, R. Güsten, J. Stutzki, A.G.G.M. Tielens

[C II] 158 μm emission

- [C II] fine-structure line one of the brightest far-infrared cooling lines of the ISM, $\sim$ 1% of total FIR continuum
- dominant cooling line of warm, intermediate density gas ($T \sim$ 50-300 K, $n \sim 10^3$-10^4 cm^{-3})
- [C II] line can be observed in distant galaxies
- origin of [C II] emission: dense PDRs, cold H I gas, ionized gas, CO-dark gas
- need to spatially resolve the ISM
- Orion molecular cloud as template region
- ideally, velocity-resolved mapping allows to form a 3D picture
- last but not least, the [C II] line is an excellent tracer of stellar feedback

Stellar feedback

- stellar feedback regulates the evolution of galaxies
- stellar winds of massive stars blow large bubbles
- slightly less massive stars create expanding H II regions
- negative feedback: hinder star formation due to cloud destruction
- positive feedback: triggered star formation in swept-up shells

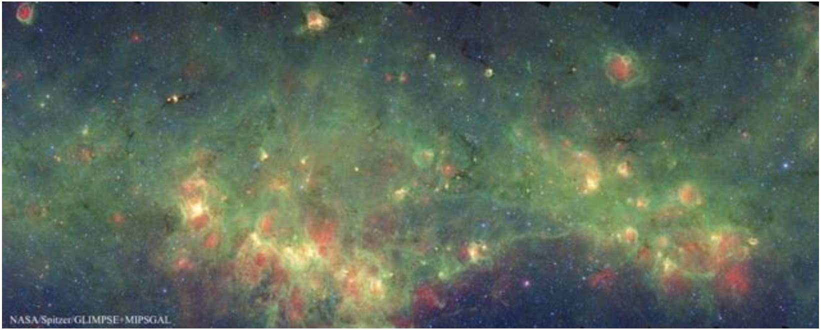

The C^+ Square-Degree (C+SQUAD)

- large-scale mapping project in the Orion A molecular cloud
- area of $1.1^\circ \times 1.4^\circ$ centered on the Orion Nebula
- velocity-resolved observations of the [C II] line with SOFIA/upGREAT
- 13 flights in November 2016 and February 2017
- resulting in 2 million spectra

Zooming into the constellation of Orion

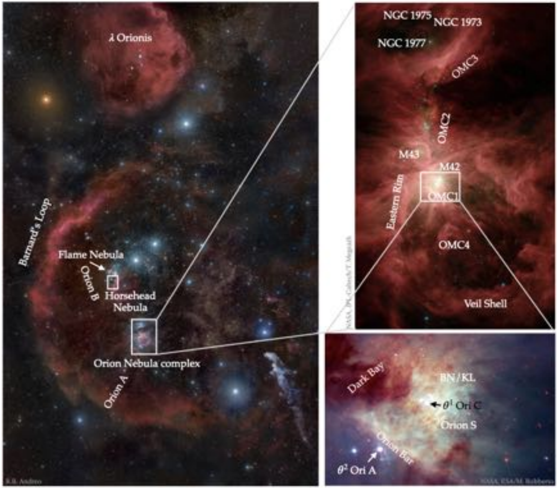

Figure 1: *Left:* Photograph of the constellation of Orion. The Horsehead Nebula and the Orion Nebula are visible in this long-time exposure (white rectangles).

Upper right: Spitzer/IRAC multi-color image of the Orion Nebula complex. Mid-infrared wavelengths reveal dust and large molecules irradiated by star light. *Lower right:* The inner Orion Nebula, with the massive Trapezium stars, as seen by the HST. The ionized gas in this regions emits in UV and optical lines. The background PDR and the Orion Bar are mainly visible at infrared and (sub-)millimeter wavelenghts.

[C II] emission from L1630 in Orion B

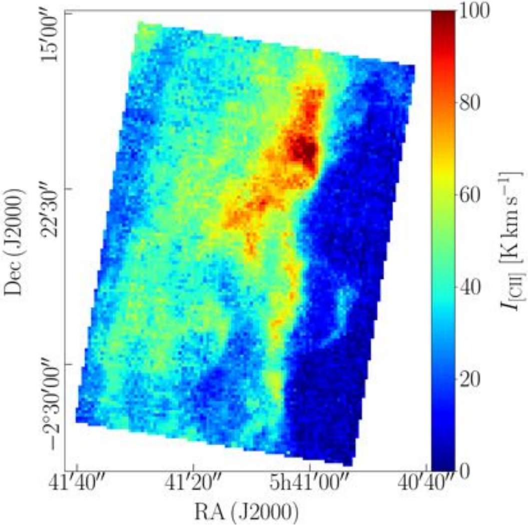

Figure 2: [C II] line-integrated intensity ($v_{\mathrm{LSR}} = 6\text{-}20\,\mathrm{km\,s^{-1}}$) observed by SOFIA/upGREAT in 2015.

Pabst et al. (2017)
Bally et al. (2018)

From small to large...

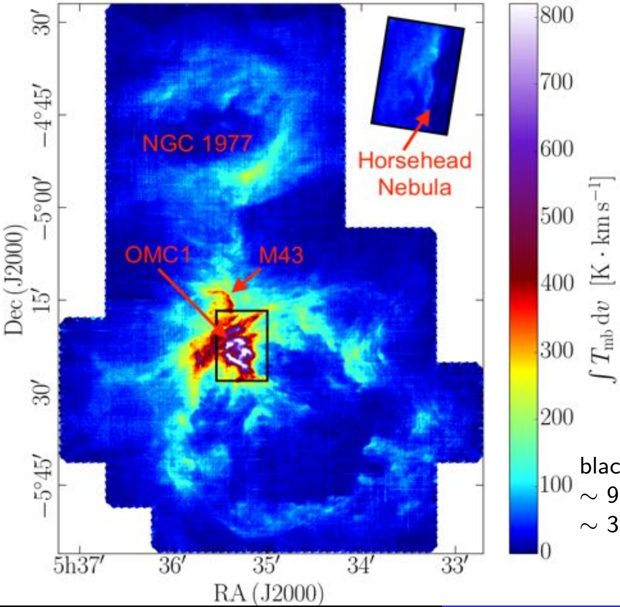

[C II] line-integrated intensity from the Orion Nebula complex

black box:
∼ 9h with *Herschel*/HIFI,
∼ 35min with SOFIA/upGREAT

upGREAT versus HIFI

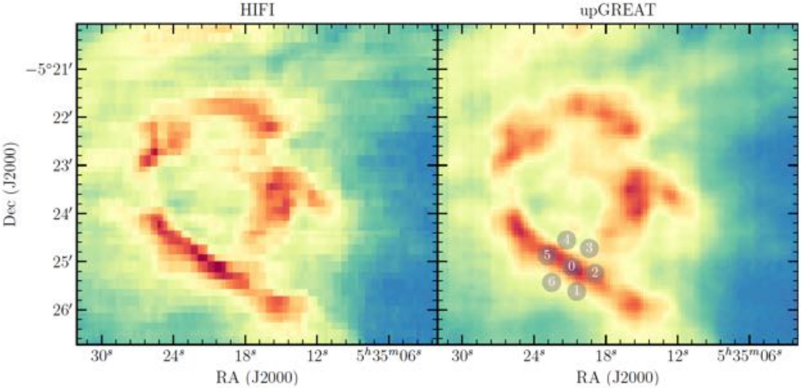

Figure 3: [C II] line-integrated intensity ($v_{\rm LSR} = -5\text{-}15\,{\rm km\,s^{-1}}$) observed by HIFI (*left*) and upGREAT (*right*). The array positions indicated in grey show the position of the Orion Bar consistency observation (Higgins et al., to be submitted).

Data reduction challenges

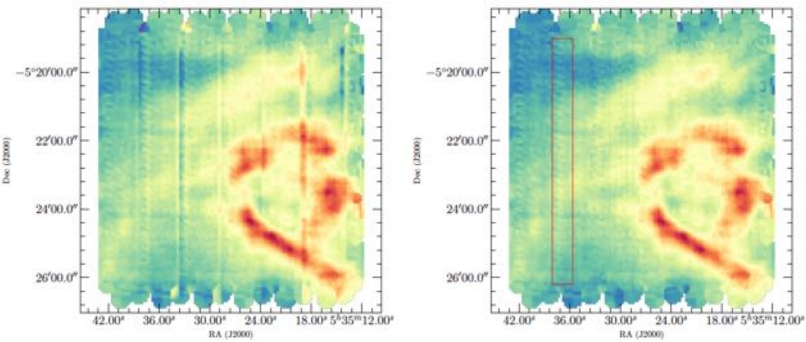

Figure 4: *Left:* Tile using a polynomial order three correction, *right:* using a spline correction approach (Higgins et al., to be submitted).

Orion's Dragon

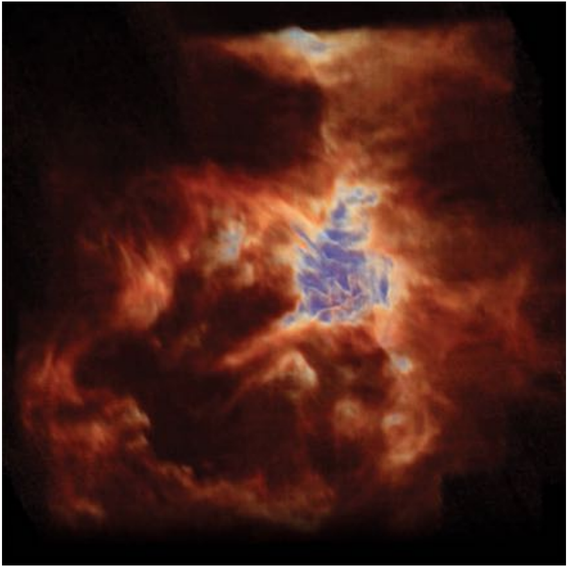

Figure 5: A screenshot from the rotating [C II] data cube observed by SOFIA/upGREAT (image credit: NASA/SOFIA).

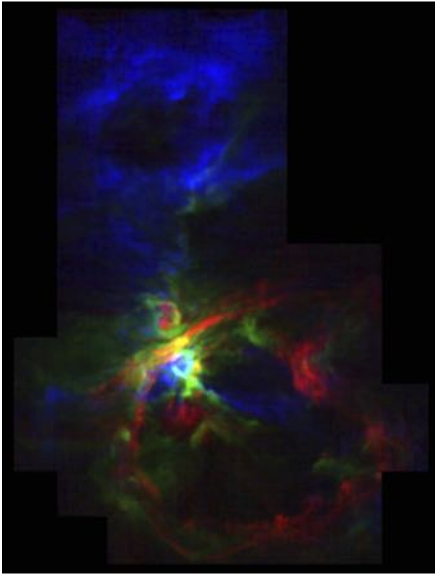

Figure 6: [C II] emission in three different velocity channels (red: $5\,\mathrm{km\,s^{-1}}$, green: $9\,\mathrm{km\,s^{-1}}$, blue: $13\,\mathrm{km\,s^{-1}}$).

Three-observatory view of the Orion Nebula

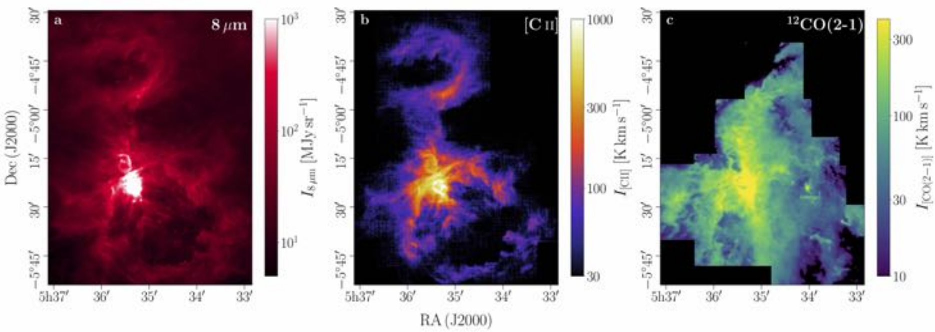

Figure 7: *(a) Spitzer*/IRAC 8 μm intensity. *(b)* SOFIA/upGREAT [C II] line-integrated intensity. *(c)* IRAM 30m ^{12}CO(2-1) line-integrated intensity.
The 8 μm emission traces FUV-irradiated PAHs in the PDR surfaces, the [C II] line is emitted by mostly neutral gas ($T \sim 100\,\mathrm{K}$), whereas CO traces the molecular gas ($T \sim 30\,\mathrm{K}$).

[C II]-FIR correlation

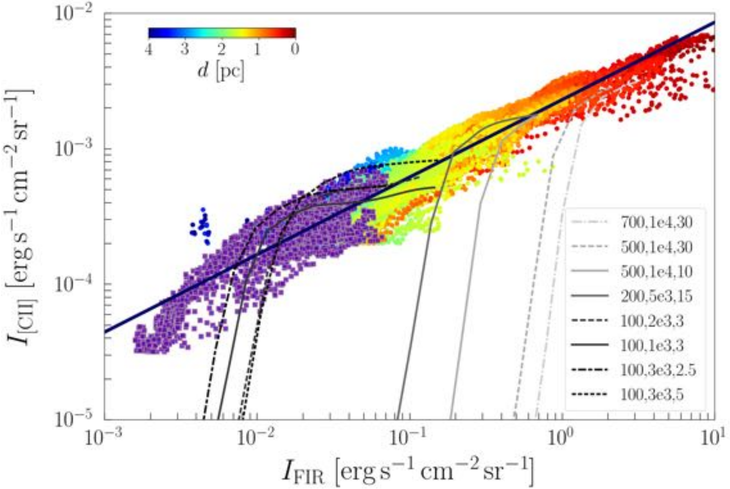

Figure 8: [C II] versus FIR intensity. Purple squares are from Orion B. The color scale in Orion A indicates distance from the Trapezium stars. Grey lines are edge-on model outputs with parameters given in the legend ($G_0, n, A_{\mathrm{V,los}}$). The blue line is a least-squares regression to the Orion A data with $\log_{10} I_{[\mathrm{CII}]} = 0.57 \log_{10} I_{\mathrm{FIR}} - 2.64$.

[C II]-8 μm correlation

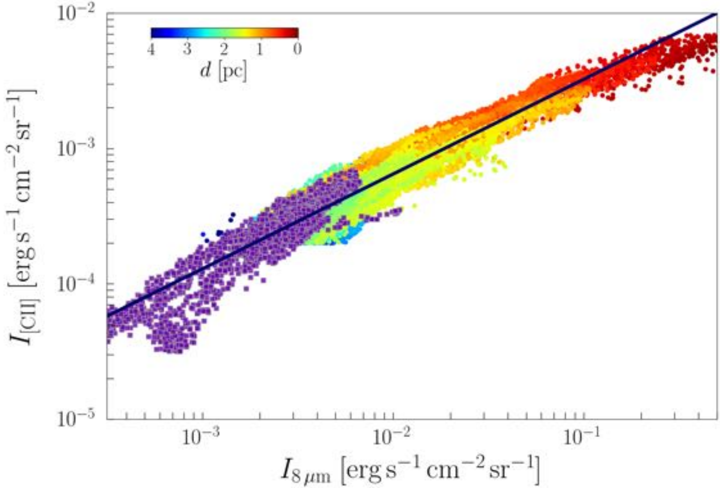

Figure 9: [C II] versus 8 μm intensity. Purple squares are from Orion B. The color scale in Orion A indicates distance from the Trapezium stars. The blue line is a least-squares regression to the Orion A data with $\log_{10} I_{[CII]} = 0.70 \log_{10} I_{8\,\mu m} - 1.79$.

Tracing expanding bubbles: The Veil Shell

Figure 10: Excess X-ray emission from the cavity of the Orion Nebula (blue). The green and red channels show the *Spitzer*/IRAC 4.5 $\mu\mathrm{m}$ and 5.8 $\mu\mathrm{m}$ emission, respectively (Güdel et al. 2008).

Tracing expanding bubbles: The Veil Shell

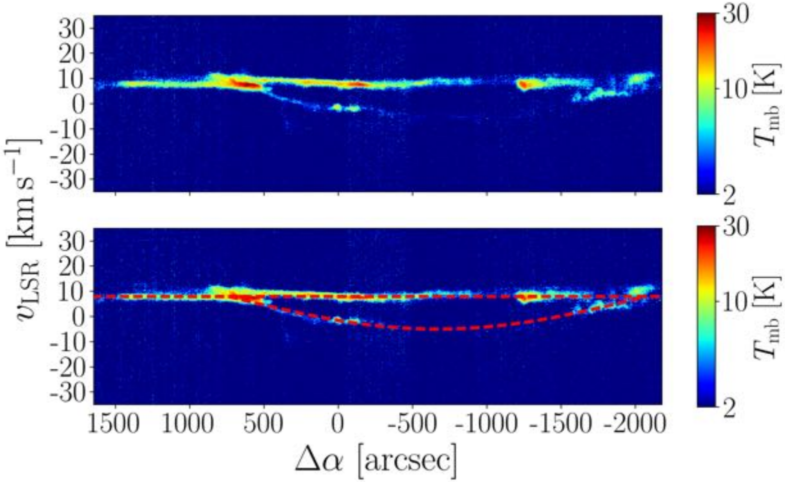

Figure 11: Position-velocity diagram of [C II] emission from the Orion Nebula. The lower panel indicates the arc structure of a spherically expanding bubble with $v_{\rm exp} = 13\,\mathrm{km\,s^{-1}}$ on a background velocity of $8\,\mathrm{km\,s^{-1}}$ (red dashed lines).

Tracing expanding bubbles: The Veil Shell

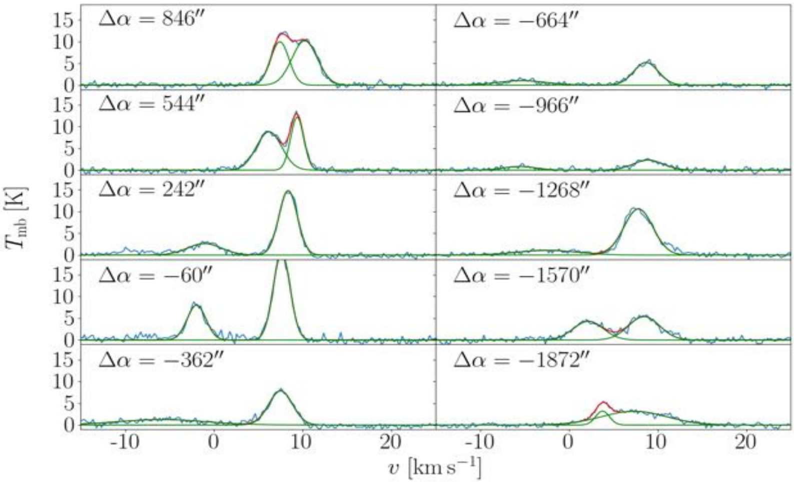

Figure 12: [C II] spectra in the Veil along previous pv diagram with Gaussian fits. Each spectrum is averaged over $(2\times)75.5'' \times 75.5''$.

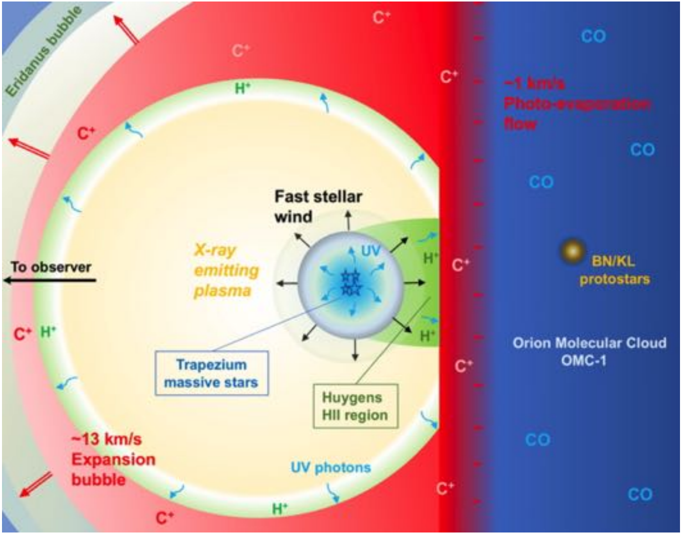

Figure 13: Schematic of the wind-blown bubble in the Orion Nebula, created by θ^1 Ori C (Pabst et al. 2019). The geometry of the Huygens Region is not rendered in its full complexity.

The 3D structure of the Orion Nebula

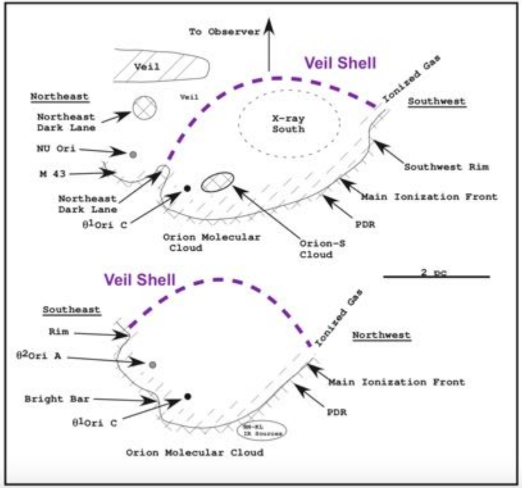

Figure 14: Geometry of the Orion Nebula (adapted from O'Dell&Harris 2010). The purple line indicates the Veil Shell.

The 3D structure of the Huygens Region

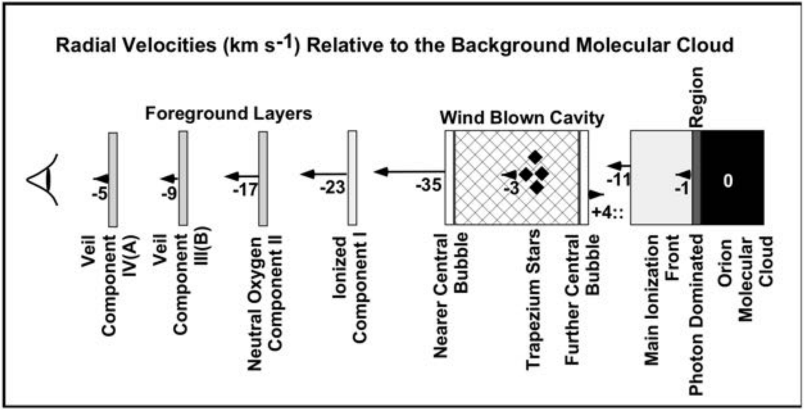

Figure 15: Velocity structure of Orion's Veil towards the Trapezium stars (Abel et al. 2019). Veil Component III(B) corresponds to the large shell.

Relevant publications

- Güdel et al. 2008, Science 319, 309
- Pabst et al. 2019, Nature 565, 618
- Abel et al. 2019, ApJ 881, 130
- O'Dell et al. 2020, ApJ 891, 64
- Pabst et al. 2020, A&A 639, A2
- Goicoechea et al. 2020, A&A 639, A1

Onwards! More bubbles:

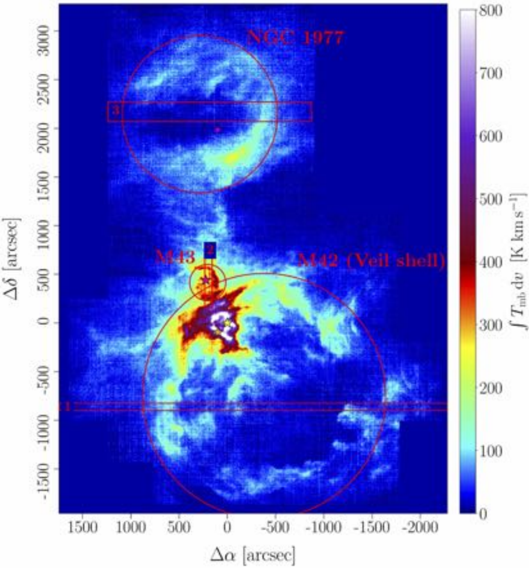

Figure 16: [C II] line-integrated intensity. Red rectangles indicate the cuts along which the pv diagrams are extracted.

Tracing expanding bubbles: The M43 Shell

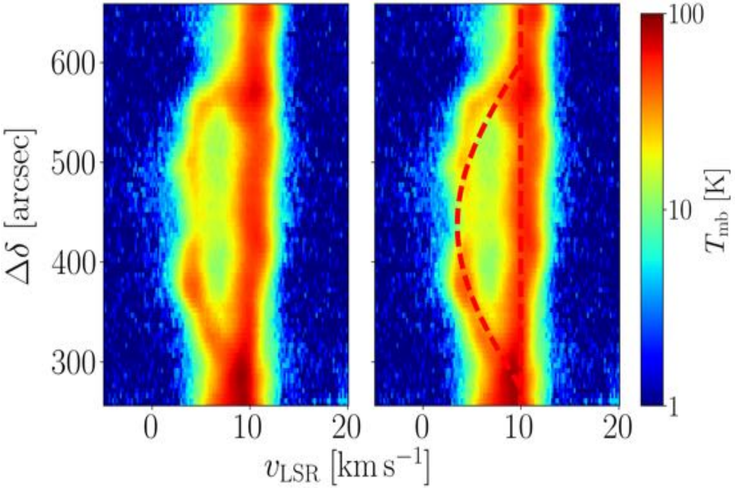

Figure 17: [C II] pv diagram through M43. The right panel shows the same pv diagram with the arc structure for an expansion velocity of 6.5 $\mathrm{km\,s^{-1}}$ on a background velocity of 10 $\mathrm{km\,s^{-1}}$ (red dashed lines).

Tracing expanding bubbles: The M43 Shell

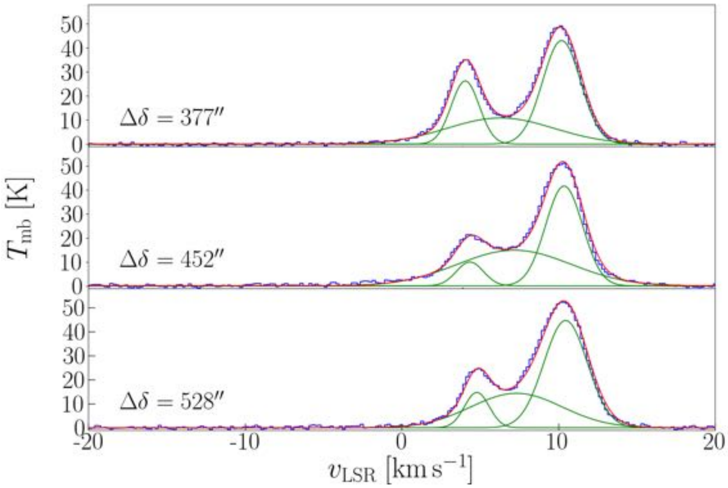

Figure 18: [C II] spectra in M43 along previous pv diagram with Gaussian fits. Each spectrum is averaged over $75.5'' \times 75.5''$.

Tracing expanding bubbles: The NGC 1977 Shell

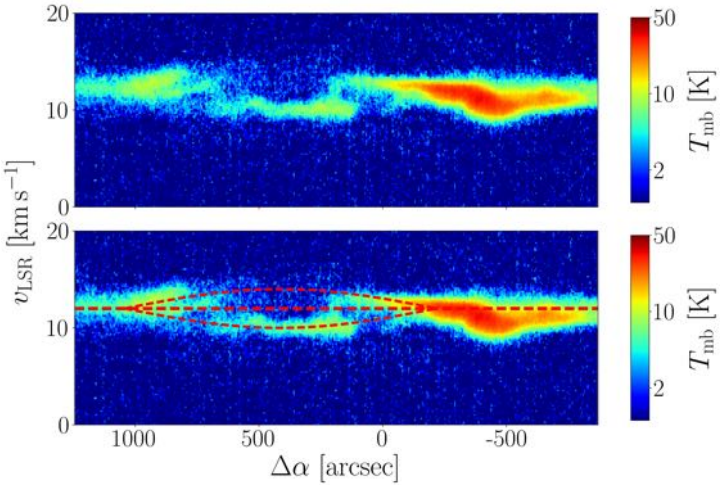

Figure 19: [C II] pv diagram through NGC 1977. The lower panel shows the same cut with the arc structure for an expansion velocity of $\pm 2\,\mathrm{km\,s^{-1}}$ (red dashed lines).

Tracing expanding bubbles: The NGC 1977 Shell

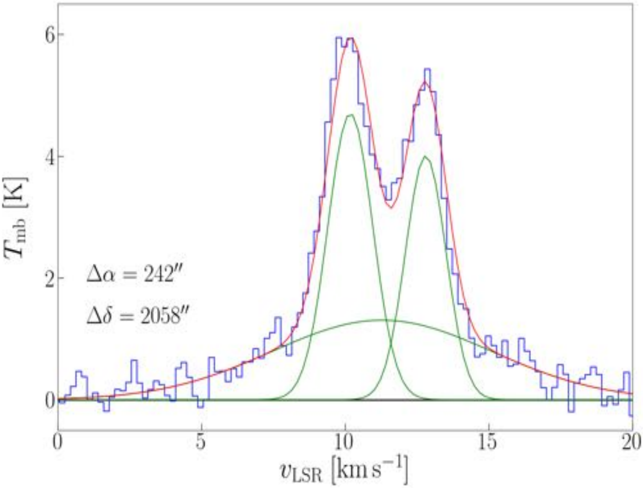

Figure 20: [C II] spectrum in NGC 1977 along the previous pv diagram with Gaussian fits, averaged over $200'' \times 200''$.

Comparison of the pressure terms

region		n [cm^{-3}]	$T_{\rm gas}$ [K]	$p_{\rm th}/k_{\rm B}$ [cm^{-3} K]	G_0
Veil Shell	plasma	0.3	2×10^6	1×10^6	
	H II	50	8×10^3	8×10^5	
	PDR	10^3-10^4	~ 100	1-10 $\times 10^5$	~ 100
M43	H II	500	7.5×10^3	8×10^6	
	PDR	10^4	100	1×10^6	$\sim 1 \times 10^3$
NGC 1977	H II	40	$\sim 10^4$	$\sim 8 \times 10^5$	
	PDR	10^3	90	9×10^4	~ 100

Table 1: Physical conditions of respective H II region and adjacent limb-brightened PDR shell in M42, M43, and NGC 1977. The density of the M42 H II region given here is appropriate for the southern EON, as is G_0 in the Veil Shell PDR.

In the Veil Shell, the plasma pressure can drive the expansion. In M43 and NGC 1977, the pressure of the ionized gas drives the expansion.

Comparison of the PDR pressures

p/k_{B}	Veil Shell	M43	NGC 1977
thermal	1-10 $\times 10^5$	1×10^6	9×10^4
magnetic	2×10^6	–	–
turbulence	0.5-3 $\times 10^6$	8×10^5	8×10^4
radiation	1×10^5	3×10^6	8×10^4

Table 2: Comparison of the pressure terms in the PDRs of the Veil Shell, M43 and NGC 1977. In the Veil Shell, higher pressures correspond to the limb-brightened edges, while lower pressures apply to the foreground expanding shell.

In the PDRs, approximate equipartition holds between the pressure terms. Radiation pressure is less important in the Veil Shell.

Comparison of the energetics

region	M42 (Veil)	M43	NGC 1977
star	θ^1 Ori C	NU Ori	42 Ori
stellar type	O7V	B0.5V	B1V
$\mathbb{N}_{\rm Lyc}$ $[10^{47}\,{\rm s}^{-1}]$	70	1.5	1
$L_{\rm w}$ $[L_\odot]$	350	$\sim 1.5 \times 10^{-2}$	$\sim 1.5 \times 10^{-2}$
mass of neutral gas $[M_\odot]$	1500	8	700
mass of ionized gas $[M_\odot]$	24	0.3	16
$v_{\rm exp}$ $[{\rm km\,s^{-1}}]$	13	6	1.5
$E_{\rm kin}$ of neutral gas $[10^{46}\,{\rm erg}]$	250	0.3	2
$E_{\rm th}$ of ionized gas $[10^{46}\,{\rm erg}]$	3	0.7	5
$t_{\rm exp}$ $[{\rm Myr}]$	0.2	0.02	0.4
$E_{\rm kin}/(L_{\rm w}\,t_{\rm exp})$	0.5	50	40

Table 3: In M42, the kinetic energy of the neutral shell much exceeds the thermal energy of the ionized gas, while the wind luminosity is sufficient to drive the expansion. In M43 and NGC 1977, the thermal energy of the ionized gas exceeds the kinetic energy of the shell, indicative of pressure-driven expansion.

Summarizing the energetics

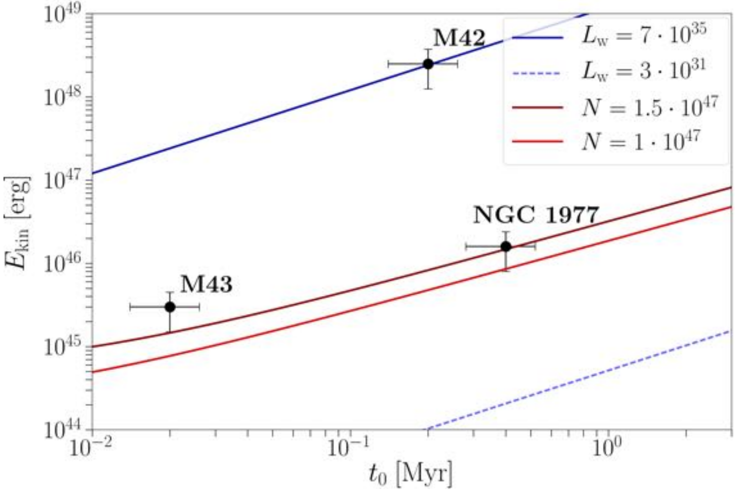

Figure 21: Kinetic energy of the expanding bubble shells versus expansion time. The lines are the predictions of wind models (blue) and models of pressure-driven expansion (red) with parameters adequate to the studied regions.

The IRAM 30m Large Program

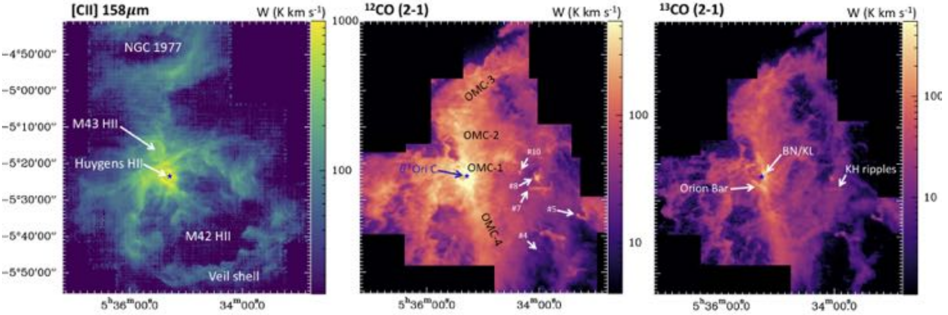

Figure 22: [C II], ^{12}CO(2-1), and ^{13}CO(2-1) emission from the Orion Nebula complex. [C II] emission traces the cloud surfaces, while CO(2-1) emission traces the molecular background cloud (Goicoechea et al. 2020).

Molecular globules in the shell

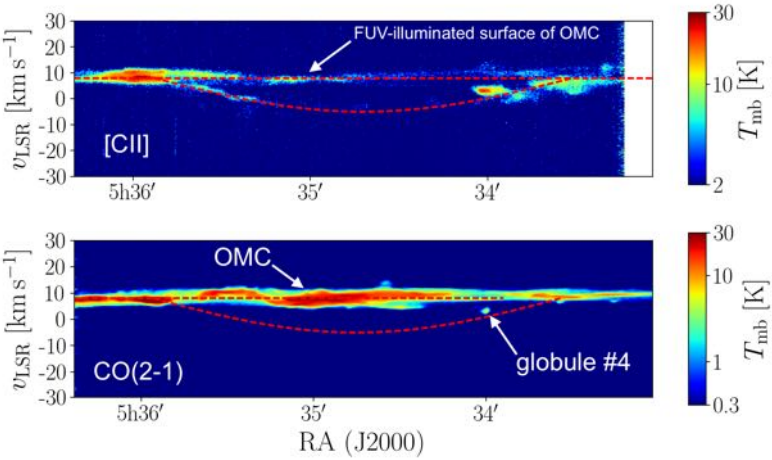

Figure 23: Position-velocity diagram of [C II] and $^{12}CO(2\text{-}1)$ emission from the Orion Nebula (Goicoechea et al. 2020).

Gallery of globules

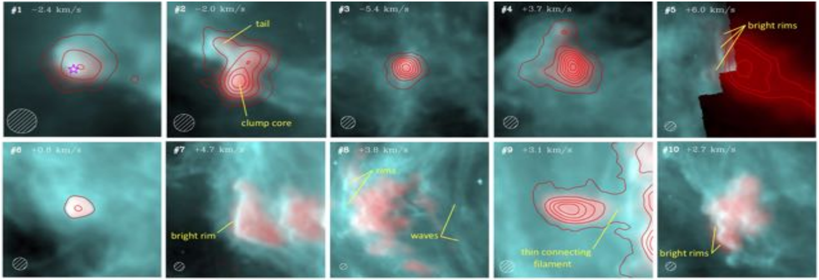

Figure 24: Blueshifted CO globules and emission structures detected toward the Veil Shell. Reddish color: ^{12}CO(2-1) emission, bluish color: IRAC 8 μm emission (Goicoechea et al. 2020).

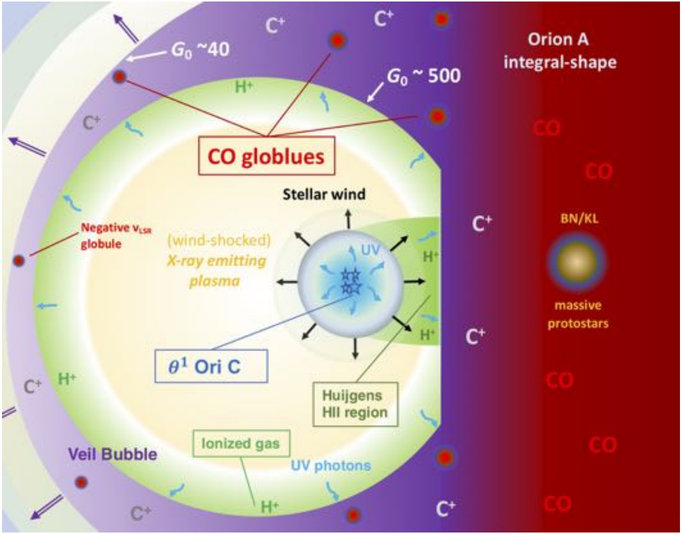

Figure 25: Schematic of the wind-blown bubble in the Orion Nebula with molecular globules (Goicoechea et al. 2020).

Summary and outlook

- The first large-scale velocity-resolved [C II] map of the Orion Nebula reveals the large-scale expansion of the Veil, that carries a large portion of the gas mass
- Other parsec-scale bubbles are observed in M43 and NGC 1977.
- While the expansion of the M42 Veil is driven by the stellar wind of θ^1 Ori C, the expansion of M43 and NGC 1977 is due to the overpressurized gas in the H II region.
- Velocity-resolved [C II] observations are a powerful tool to quantify stellar feedback from massive stars
- SOFIA/upGREAT is the prime facility because of its high mapping speed
- Role of magnetic fields in bubble expansion?
- SOFIA Legacy Program FEEDBACK: 11 sources

The SOFIA Legacy Program FEEDBACK

- PIs: Nicola Schneider & Alexander Tielens
- Science goal: How do massive stars regulate star formation?
- Survey of 11 regions of massive star formation in the [C II] line using upGREAT on SOFIA. The sample spans a wide range in star formation characteristics and physical conditions.
- The data is non-proprietary.
- About 30% complete as of August 2020